Journal of Stress Analysis
Vol. 4, No. 2, Autumn – Winter 2019-20
Bu-Ali Sina University

Continuum Damage Mechanics for Creep Lifetime Estimation in Polymer Matrix Composites at Various Temperatures

H. Bahmanabadi, M. Azadi*, K. Keypour
Faculty of Mechanical Engineering, Semnan University, Semnan, Iran.

Article info

Article history:
Received 19 September 2019
Received in revised form
26 November 2019
Accepted 19 January 2020

Keywords:
Creep lifetime prediction
Polymer matrix composites
Continuum damage mechanics
Levenberg-Marquardt method

Abstract

Nowadays, composites have great applications in mechanical structures due to their proper ratio of the strength to the weight. Such application includes automotive and aerospace industries. These components may be affected by the creep phenomenon, when they work at high temperatures. Therefore, there should be appropriate creep behavior of materials for these parts. In this article, the Continuum Damage Mechanics (CDM) method was used to calculate the creep lifetime of various polymer matrix composites. For this objective, experimental data were utilized from creep tests in the literature, on standard specimens, at different temperatures. Then, the relation between the stress, the temperature and the lifetime was presented by the CDM approach, which was calibrated by experimental results. In addition, the Levenberg-Marquardt method was employed to optimize the creep lifetime equation and to find temperature-dependent material constants. Consequently, the obtained results showed that there was a good agreement between experimental and calculated creep lifetimes of composites.

Nomenclature

k, A, r	Temperature-dependent material constants	σ	Stress
t_{cr}	Critical creep lifetime	D_0	Initial damage
D_{cr}	Critical damage	F	Vector-valued function
T	Matrix transpose	$\nabla f(x)$	F Gradient
x_*	The solution of the least square problem		

1. Introduction

Composite materials have been widely used in various industries, such as automotive, aerospace, and civil engineering, as well as other industries. Since high ratios of the strength to the weight have a great importance to designers, In recent years, fiber-reinforced polymer composites have found applications in such industries.

Polymers and polymer composites are viscoelastic in nature. The creep phenomenon is a time-dependent behavior of materials, whereby a constant stress is applied and the resulting strain is characterized. The study of polymer composites necessitates the evaluation of such viscoelastic behavior at various frequencies and different temperatures. The viscoelastic behavior is best demonstrated by creep and stress relaxation tests.

Along with experiments, modeling had an impor-

*Corresponding author: M. Azadi (Assistant Professor)
E-mail address: m_azadi@semnan.ac.ir
http://dx.doi.org/10.22084/jrstan.2020.20090.1114
ISSN: 2588-2597

tant role in designing. One method is the Continuum Damage Mechanics (CDM) approach. As an advantage of this model, the creep damage could be predicted during the time. Knowing the damage behavior of materials can help engineers for an appropriate design of mechanical structures under creep loading [1-3]. There are several researches about the creep rupture of polymeric composites. A literature review is performed in the following paragraphs.

Chevali et al. [4] studied the flexural creep behavior of nylon, polypropylene, and high-density polyethylene long fiber thermoplastic composites. They indicated that all materials had non-linear viscoelasticity behaviors with a good creep resistance. Eftekhari and Fatemi [5] investigated the creep behavior of neat, talc-filled, and short glass fiber reinforced injection molded thermoplastic composites, besides modeling at elevated temperatures. The creep strength decreased and the creep strain and the creep rate increased by increasing the temperature. They showed that the temperature effect was more significant for samples with glass fibers in the transverse to the load direction, as compared to the longitudinal direction. Rwawiire et al. [6] characterized the global surge in the application of natural fiber reinforced polymer composites in various industries. Their results indicated that the creep behavior was affected by the layering pattern of laminar composites. Du et al. [7] evaluated the creep response of laboratory-made natural fiber-reinforced thermoset polymer composite face/honeycomb core sandwich panels and compared them to those of relevant sandwich-structure composites, studied in the literature. Song et al. [8] demonstrated the determination of the design stresses for high-temperature polymer PMR-15 and carbon fiber/PMR-15 composites. They implied that the mechanical performance of PMR-15 could be improved by adding carbon fibers. Moreover, to determine creep responses of the composite, a rule of the mixture approach was adopted.

Pulngern et al. [9] presented the effect of temperature on mechanical properties and tensile creep responses of wood/PVC composite materials. They observed closed agreement representing the accuracy of models to predict the long-term deformation of materials. Jabbar et al. [10] reported the creep behavior of alkali treated jute/green epoxy composites, incorporated with various loadings (1, 5, and 10 wt.%) of chemically treated pulverized jute fibers, at different temperatures. Dynamic mechanical thermal analysis results revealed an increase in the storage modulus and the glass transition temperature and a reduction in the tangent delta peak height of composites under higher loading. Dutta and Hui [11] evaluated tension and compression creep behaviors of glass-fiber reinforced polyester composites. They measured failure stresses at three different temperatures. Furthermore, they presented an empirical model to estimate the creep lifetime. Gupta and Raghavan [12] investigated the creep properties of plain weave polymer matrix composites under both on-axis and off-axis loading. They showed that the creep compliance was enhanced by increasing the orientation angle of the load. They also understood a significant effect of the stress and the temperature on creep behaviors under off-axis loading, higher than ones under on-axis loading. Mortazavian and Fatemi [13] found the cyclic deformation and the fatigue behavior of two short fiber thermoplastic composites, under a number of loading and environmental conditions. They represented empirical equations to characterize self-heating under cyclic loading. Additionally, the Tsai-Hill criterion was applied to account for the effect of the fiber orientation on the fatigue lifetime. Ghosh et al. [14] characterized graphene-based nano-reinforcements as promising fillers in polymeric materials. Their thermal analyses indicated reduction in the glass transition temperature of the composite, whereas no significant impact was observed on the decomposition temperature. The creep resistance was improved at relatively lower temperatures and stresses.

Pegoretti and Ricco [15] characterized the creep crack propagation in a short glass fiber reinforced polypropylene composite at various temperatures. They showed that the crack speed decreased firstly to a minimum value and then, had a steady behavior, which was influenced by the temperature. Su et al. [16] conducted creep tests on C/SiC composites, with and without protective layers, under various stresses and temperatures, in the hot oxidizing atmosphere. They concluded that the creep mechanism of C/SiC composites was due to and controlled by the oxidation/ablation of carbon fibers. Cano-Crespo et al. [17] investigated the high-temperature creep behavior of carbon nanofiber-reinforced and graphene oxide-reinforced alumina composites. They found that graphene-oxide reinforced alumina composites had higher creep resistant than that of carbon nanofibers-reinforced alumina ones or monolithic alumina with the same grain size distribution. In all cases, grain boundary sliding was identified as the deformation mechanism. Plaseied and Fatemi [18] studied the tensile creep behavior of the vinyl ester polymer and its nanocomposite. Their results demonstrated that at lower temperatures, higher creep compliance was observed for vinyl ester, comparing to the nanocomposite. Hung et al. [19] found the effect of the wood acetylation on mechanical properties and the creep resistance of wood/recycled-polypropylene composites using the time-temperature superposition principle. Their results revealed that flexural and tensile strengths increased by increasing the weight percent gain of acetylated wood particles, up to 13%. Raghavan and Meshii [20] developed a creep model to estimate the creep of carbon fiber-reinforced composites. They illustrated a good capability of the presented creep model for uni-

directional composites. Militky and Jabbar [21] presented the short-term creep behavior of novel treated jute fabric reinforced green epoxy composites. Dynamic mechanical analysis results showed a reduction in the tangent delta peak height of the treated composites, which might be due to the improvement in the fiber/matrix interfacial adhesion.

Based on the literature review, researches about the CDM approach for modeling of the creep lifetime in materials are still infrequent. Therefore, this article presents the creep lifetime prediction in polymer matrix composites at different temperatures using CDM models. The obtained results are shown in tables and figures.

2. Materials and Methods

2.1. Specimens

Different thermoplastics in the matrix phase, the talc and the glass fiber in the reinforcement phase were used for the composite production, based on the literature [5]. A summary of materials utilized in this study, including constituents, the polymer matrix, and the reinforcement are presented in Table 1. More details of the production could be found in the literature [5]. Some properties and other test conditions such as the melting temperature (T_m), the glass transition temperature (T_g), the loading direction, the stress level, and the temperature are presented in Table 2.

In Table 2, the letter "L" shows the longitudinal direction (fibers along with load directions) and the letter "T" shows the transverse direction (fibers perpendicular to load directions). For better understanding, the direction and the location of specimens are also shown in Fig. 1.

It should be noted that the mean glass fiber length and the diameter for reinforced composites with glass fibers were 0.25mm and 10μm, respectively [5].

2.2. Creep Tests

Creep tests were conducted by Eftekhari and Fatemi [5], using a closed-loop servo-hydraulic test machine with the digital controller, based on the ASTM-D2990 standard [22]. A video extensometer was utilized to measure the creep strain. A pair of pneumatic grips, with 5kN of the capacity and the adjustable pressure system was used, which could be appropriate for low- and high-temperature polymer tests.

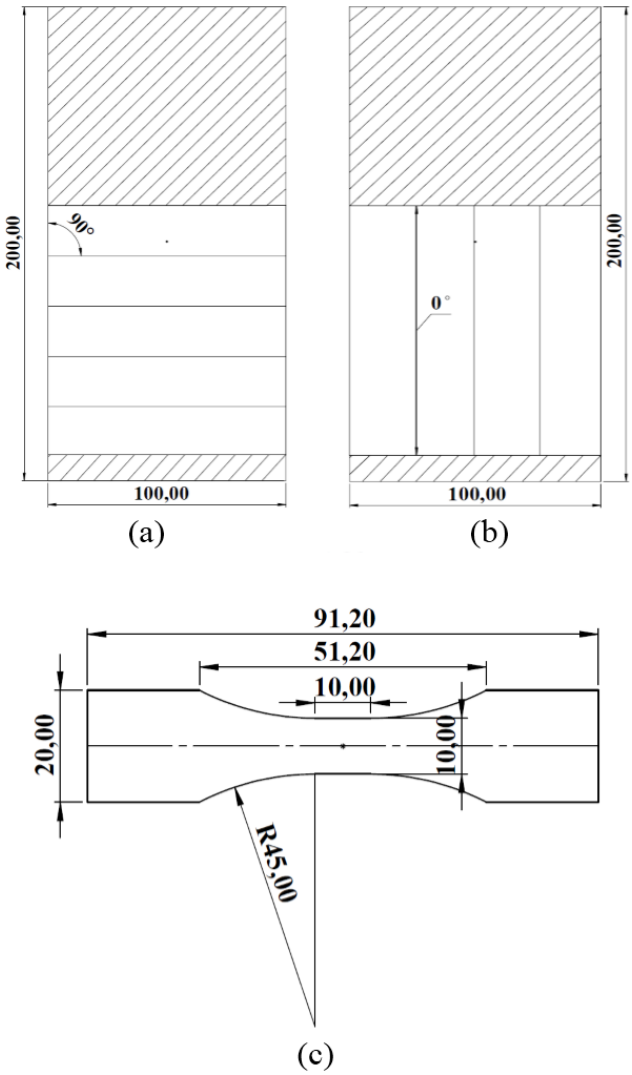

Fig. 1. The direction and the location of specimens, in a) The transverse direction and b) The longitudinal direction, according to the mold flow direction (arrows), and c) The specimen geometry used for creep tests (dimensions are in mm) [5].

Table 1
Materials used in creep tests [5].

Material	Matrix	Reinforcement
PO	Polypropylene+25 wt.% Rubber	30 wt.% Talc
PP	Impact Polypropylene	None
PP-T	Polypropylene	40 wt.% Talc
PP-G	Polypropylene	30 wt.% Short glass fiber
PA66	Polyamid-6,6	30 wt.% Short glass fiber
PPE/PS	Polyphenylene Ether+Polystyrene	30 wt.% Short glass fiber
PBT	Polybutylene terephthalate	30 wt.% Short glass fiber
PA6	Polyamide-6+10% Rubber	30 wt.% Short glass fiber

Table 2
Properties and creep test conditions of the material [5].

Material	T_m (°C)	T_g (°C)	Direction	T (°C)	σ (% S_u)
PO	>120	<-10	T	23-125	20-82
PP	170	4	T	23-125	40-85
PP-T	165	11	T	23, 85	53-80
PP-G	165	23	T	23-120	46-85
PA66	260	55	T	23-120	75-90
PPE/PS	325	135	T	23, 85	60-85
PBT	255	50	T, L	85, 125	72-91
PA6	220	40	T, L	85, 125	81-91

2.3. Continuum Damage Mechanics

The CDM is a way to calculate the cumulative damage. It is a useful instrument to model the effect of the damage propagation.

The CDM estimates the creep lifetime by introducing a damage function. The creep damage evaluation can be expressed with a single damage state variable, in the creep lifetime estimation model. Eq. (1) shows the creep damage evaluation [23].

$$dD_c = \left(\frac{\sigma}{A}\right)^r (1 - D_c)^{-k} dt \tag{1}$$

where k, A, and r are temperature-dependent material constants.

The creep lifetime until the final rupture is expressed by t_r and it could be achieved by an integration of Eq. (1), from boundaries between $D_c = D_0$ and $D_c = D_{cr}$ and also from $t = 0$ to $t = t_{cr}$ [23], as follows,

$$t_{cr} = \frac{1}{k+1}[(1 + D_0)^{k+1} - (1 - D_{cr})^{k+1}] \left[\frac{\sigma}{A}\right]^{-r} \tag{2}$$

It should be noted that $D_0 = 0$ and $D_{cr} = 1$, in this research. The creep damage evaluation could be expressed by Eq. (3) [23].

$$D_c = 1 - \Bigg\{(1 - D_0)^{k+1} - [(1 - D_0)^{k+1} - (1 - D_{cr})^{k+1}]\frac{t}{t_{cr}}\Bigg\}^{\frac{1}{k+1}} \tag{3}$$

where D_0 and D_{cr} represent the initial damage and the critical damage, respectively [23].

It should be noted that there were some limits in CDM modeling. One limit was that there was no parameter to show the temperature effect on the creep lifetime. To solve such a problem in this research, the relation between three parameters (k, A, and r) and the temperature was obtained by curve-fitting in the last part of the article. This consideration could be mentioned as a novelty of this article. Another limit of CDM modeling was that there was no parameter to consider the effect of the activation energy for the creep phenomenon. However, such a parameter was not evaluated in this research.

2.4. Levenberg-Marquardt Method

As mentioned, there are three temperature-dependent material constants in creep lifetime estimation equations. To obtain these constants, the CDM equation, Eq. (2), should be optimized. The Levenberg-Marquardt method is a nonlinear least square method, which could be utilized for the optimization. A minimization problem could be written as follows [23],

$$\min_m : f = \frac{1}{2}\sum_{i=1}^{m} f_i(x)^2 \equiv \frac{1}{2}F(x)^T F(x) \tag{4}$$

where F is the vector-valued function, as follows [23],

$$F(x) = (f_1(x) \quad f_2(x) \quad \cdots \quad f_m(x))^T \tag{5}$$

The component $\nabla f(x)$ could be derived, as follows [23],

$$\nabla^2 f(x) = \nabla F(x) F(x) \tag{6}$$

$\nabla^2 f(x)$ could be derived by differentiating Eq. (6), with respect to x_j, as follows [23],

$$\nabla^2 f(x) = \nabla F(x) F(x)^T + \sum_{i=1}^{m} f_i(x) \nabla^2 f_i(x) \tag{7}$$

Now, x_* is the solution of the least square problem of $f(x_*) = 0$. Then, $f_i(x_*) = 0$ for all i, indicates that all residuals are zero and the obtained model has a good agreement with data, with small errors. Therefore, $F(x_*) = 0$ and hence, $\nabla f(x_*) = 0$, which confirms that the first-order necessary condition is satisfied [23].

$$\nabla^2 f(x_*) = \nabla F(x_*) F(x_*)^T \tag{8}$$

If $\nabla F(x_*)$ is a full-rank matrix and $\nabla^2 f(x_*)$ is a positive definite matrix [23].

The MathWorks MATLAB software was used to find the temperature-dependent material constants, in this research, due to complex optimization equations. At first, input values such as stress levels, experimental creep lifetimes, initial and critical damages were added to the software as a matrix. The Levenberg-Marquardt method was called and each parameter got the initial value. Finally, the equation would be optimized.

3. Results and Discussion

As mentioned, creep tests were conducted on some types of composites at different temperatures and stress levels. Composites were the thermoplastic resin matrix reinforced by talc and short glass fibers. The creep lifetime was predicted using CDM models to compare to experimental data. It is notable that in all optimization theories, the initial damage was considered as zero and the critical damage was considered as a unity.

3.1. PO Composites

This composite had polypropylene and rubber in the matrix and talc in the reinforcement phase. Creep tests were conducted at 23°C, 85°C, and 125°C, under different stress levels. Creep test details, including experimental and predicted creep lifetimes and also average relative errors are presented in Table 3. According to data presented in Table 3, average relative errors for differences between experimental and the predicted creep lifetimes for PO composites, at 23°C, 85°C, and 125°C were 21.90%, 41.53%, and 26.55%, respectively. Maximum relative errors were 59.29%, 83.86%, and 34.81% at 23°C, 85°C, and 125°C, respectively. These values seemed to be in a proper range, where all errors were lower than 84%. Fig. 2 shows the creep damage evaluation versus the normalized time for PO composites at different temperatures. During testing, higher damages occurred at 23°C, in comparison to those of other temperatures, maybe due to the complex temperature-dependent viscoelastic behavior. Experimental and predicted creep lifetimes, within the 2X scatterband for PO specimens, are also presented in Fig. 3.

3.2. PP Composites

These composite specimens were consisting of impact polypropylene, without reinforcements. Creep test details for PP specimens are presented in Table 4. As shown in Table 4, the average relative errors for the differences between experimental and predicted creep lifetimes of PP composites at 23°C, 85°C, and 125°C were obtained as 19.45%, 13.12%, and 17.25% and maximum relative errors were calculated as 59.07%, 23.01%, and 21.21%, respectively.

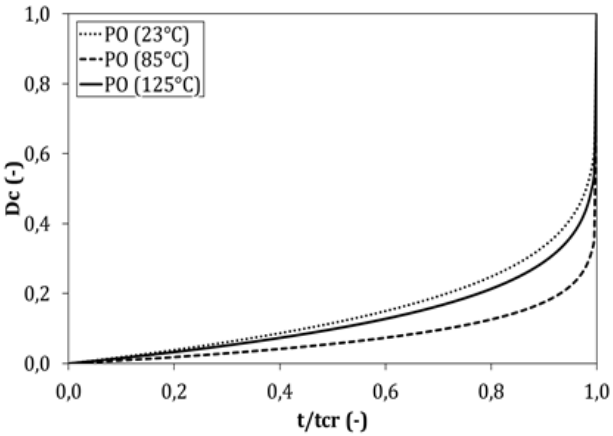

Fig. 2. The creep damage evaluation versus the normalized time for PO composites at different temperatures.

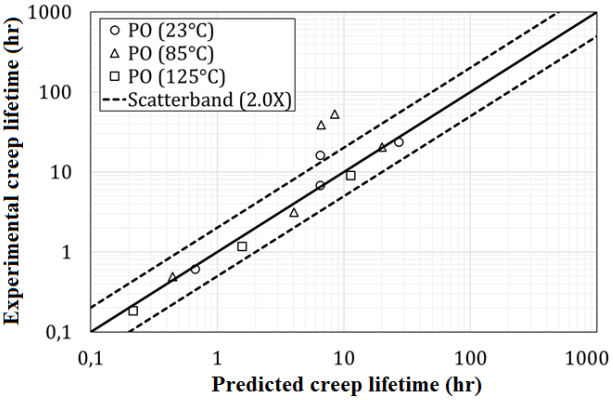

Fig. 3. The experimental creep lifetime versus the predicted creep lifetime for PO composites at different temperatures.

Table 3
Creep test conditions for PO composites.

T (°C)	σ (MPa)	Experimental lifetime [3] (hr)	Predicted lifetime (hr)	Error (%)
23	11.96	0.61	0.67	9.72
23	10.00	6.79	6.54	3.73
23	10.00	16.05	6.54	59.29
23	8.94	23.65	27.16	14.86
85	2.99	0.49	0.44	9.78
85	2.00	3.13	4.05	29.46
85	1.83	38.80	6.62	82.93
85	1.75	52.44	8.47	83.86
85	1.50	20.34	20.01	1.64
125	1.46	0.18	0.22	18.75
125	0.96	1.16	1.57	34.81
125	0.63	8.98	11.32	26.09

Table 4
Creep test conditions for PP composites.

T (°C)	σ (MPa)	Experimental lifetime [3] (hr)	Predicted lifetime (hr)	Error (%)
23	18.93	1.03	0.96	6.50
23	17.91	1.98	2.07	5.12
23	16.04	7.90	9.71	22.83
23	16.04	23.71	9.71	59.07
23	13.97	69.33	66.75	3.72
85	8.05	0.25	0.27	8.18
85	6.03	3.42	2.63	23.01
85	4.51	23.71	25.65	8.18
125	3.93	0.33	0.27	18.23
125	2.94	0.92	1.12	21.21
125	1.97	9.01	7.90	12.31

These values seemed to be in a proper range, where all errors were lower than 59%. The creep damage evaluation versus the normalized time for PP composites at different temperatures can be seen in Fig. 4. Again, higher damages were related to the test at 23°C, in comparison to those of other temperatures. Moreover, lower damages were related to the test at 125°C. Fig. 5 demonstrates the experimental creep lifetime versus the predicted creep lifetime within the 2X scatterband for PP specimens. Only one data was out of the scatterband.

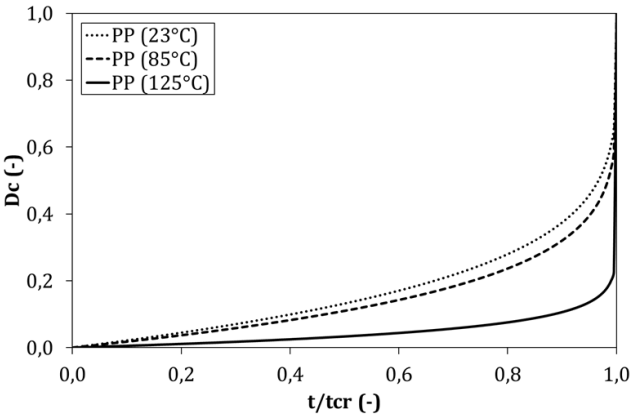

Fig. 4. The creep damage evaluation versus the normalized time for PP composites at different temperatures.

3.3. PP-T Composites

These specimens had polypropylene in the matrix and talc in the reinforcement phase. Creep tests were conducted at 23°C and 85°C under different stress levels. Creep test conditions for PP-T specimens are presented in Table 5.

According to creep test data, shown in Table 5, the average relative errors for differences between experimental and predicted creep lifetimes of PP-T composites at 23°C and 85°C were 15.66% and 12.38% and maximum relative errors were 33.30% and 22.70% , respectively. These values seemed to be in a proper range, where all errors were lower than 33% . Fig. 6 depicts the creep damage versus the normalized time for PP-T specimens, in which at different temperatures, the damage was almost the same. Experimental and predicted creep lifetimes, within the 2X scatterband for all data of PP-T specimens can be seen in Fig. 7.

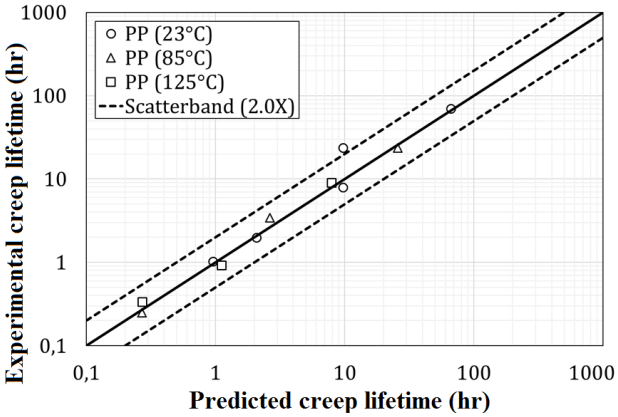

Fig. 5. The experimental creep lifetime versus the predicted creep lifetime for PP composites at different temperatures.

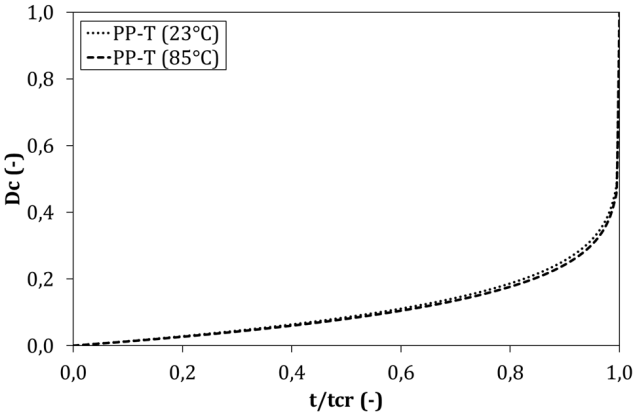

Fig. 6. The creep damage evaluation versus the normalized time for PP-T composites at different temperatures.

Table 5
Creep test conditions for PP-T composites.

T (°C)	σ (MPa)	Experimental lifetime [3] (hr)	Predicted lifetime (hr)	Error (%)
23	23.61	0.70	0.77	10.16
23	22.03	3.65	2.84	22.17
23	22.03	3.37	2.84	15.89
23	19.99	13.29	17.72	33.30
23	19.99	20.11	17.72	11.88
23	18.91	52.37	5.47	3.63
23	18.40	97.45	85.18	2.59
85	9.07	1.77	1.37	22.70
85	8.46	4.97	5.30	6.53
85	8.46	4.60	5.30	15.13
85	7.78	24.73	26.96	8.98
85	7.78	29.64	26.95	9.07
85	7.57	43.70	46.36	6.09
85	7.36	97.45	79.73	18.18

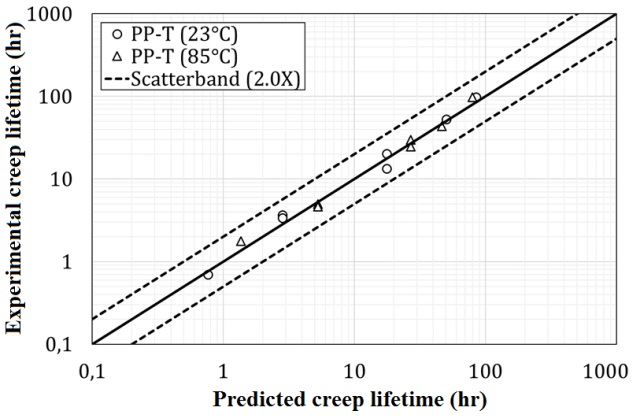

Fig. 7. The experimental creep lifetime versus the predicted creep lifetime for PP-T composites at different temperatures.

3.4. PP-G Composites

These composites had polypropylene in the matrix and the short glass fiber in the reinforcement phase. Creep tests were done at 23°C, 85°C, and 120°C under different stress levels. Creep test conditions are presented in Table 6. Fig. 8 illustrates the creep damage evaluation versus the normalized time for PP-G composites at different temperatures. At lower temperatures, lower damages occurred in the material. The experimental creep lifetime versus the predicted creep lifetime, within the 2X scatterband for PP-G specimens, is depicted in Fig. 9. The whole data were within the mentioned scatterband, which showed the accuracy of the modeling.

According to the data presented in Table 6, the average relative errors for differences between experimental and predicted creep lifetimes of PP-G composites at 23°C, 85°C, and 120°C were 12.93%, 9.57%, and 6.12% and the maximum relative errors were 22.37%, 27.73%, and 16.70%, respectively. These values seemed to be in a proper range, where all errors were lower than 28%.

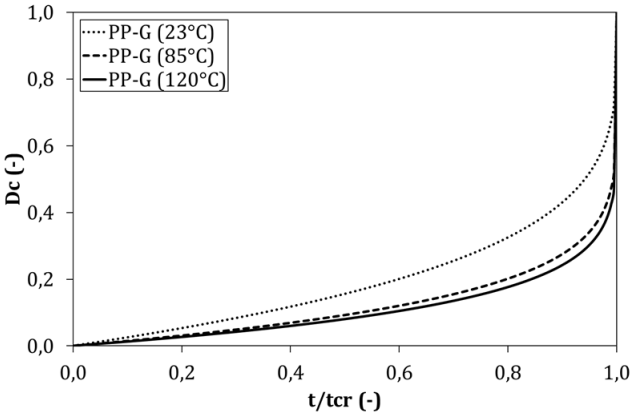

Fig. 8. The creep damage evaluation versus the normalized time for PP-G composites at different temperatures.

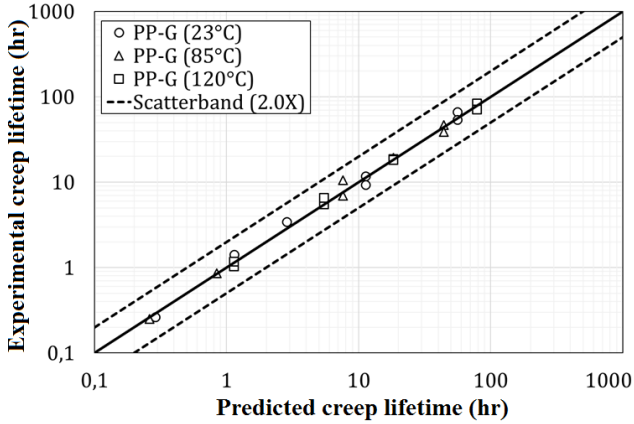

Fig. 9. The experimental creep lifetime versus the predicted creep lifetime for PP-G composites at different temperatures.

Table 6
Creep test conditions for PP-G composites.

T (°C)	σ (MPa)	Experimental Lifetime [3] (hr)	Predicted Lifetime (hr)	Error (%)
23	40.05	0.26	0.29	10.34
23	36.85	1.40	1.15	18.37
23	34.86	3.42	2.86	16.23
23	32.08	9.24	11.31	22.37
23	32.08	11.70	11.31	3.30
23	29.11	65.79	56.16	14.65
23	29.11	53.37	56.16	5.23
85	17.91	0.25	0.26	4.62
85	16.03	0.85	0.84	1.18
85	13.02	10.54	7.61	27.73
85	13.02	6.93	7.61	9.84
85	11.98	19.23	18.35	4.60
85	11.02	46.82	44.22	5.56
85	11.02	38.99	44.22	13.43
120	8.83	1.03	1.14	10.75
120	8.83	1.17	1.14	2.83
120	7.37	5.48	5.48	0.04
120	7.37	6.58	5.48	16.70
120	6.42	18.74	18.38	1.92
120	6.42	18.25	18.38	0.68
120	5.43	83.26	78.50	5.72
120	5.43	71.17	78.50	10.30

3.5. PA66 Composites

The mentioned composite had polyamide-6.6 in the matrix and the short glass fiber in the reinforcement phase. Creep tests were performed at 85°C and 120°C under different stress levels. Creep test conditions are presented in Table 7.

According to creep test details presented in Table 7, average relative errors of differences between experimental and predicted creep lifetimes at 85°C and 120°C were obtained as 21.25% and 43.97% and maximum relative errors were 58.32% and 89.06%, respectively. These values seemed to be in a proper range, where all errors were lower than 89%. Fig. 10 demonstrates the creep damage evaluation versus the normalized time for PA66 composites at different temperatures. Similar to previous results, the damage at 85°C was lower than that at 120°C. Fig. 11 shows the experimental creep lifetime versus the predicted creep lifetime, within the 2X scatterband for PA66 specimens.

3.6. PPE/PS Composites

These specimens included polyphenylene ether and polystyrene in the matrix and the short glass fiber in the reinforcement phase. Creep tests were carried out at 23°C and 85°C and under different stress levels. Creep test conditions are detailed in Table 8. According to data presented in Table 8, the average relative errors of differences between experimental and predicted creep lifetimes at 23°C and 85°C were 23.99% and 11.71% and maximum relative errors were 48.13% and 22.44%, respectively.These values seemed to be in a proper range, where all errors were lower than 48%. The curve of the creep damage evaluation versus the normalized time for PPE/PS composites at different temperatures can be seen in Fig. 12.

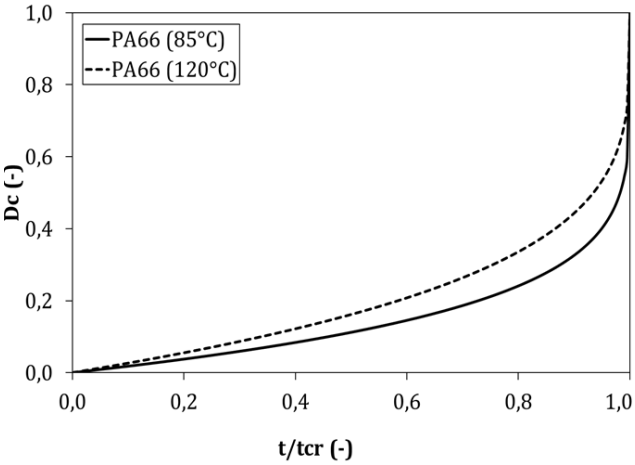

Fig. 10. The creep damage evaluation versus the normalized time for PA66 composites at different temperatures.

Based on such results, the lower temperature had higher damage. Fig. 13 shows the experimental creep lifetime versus the predicted creep lifetime, within the 2X scatterband for PPE/PS specimens. Almost all data were within the mentioned scatterband.

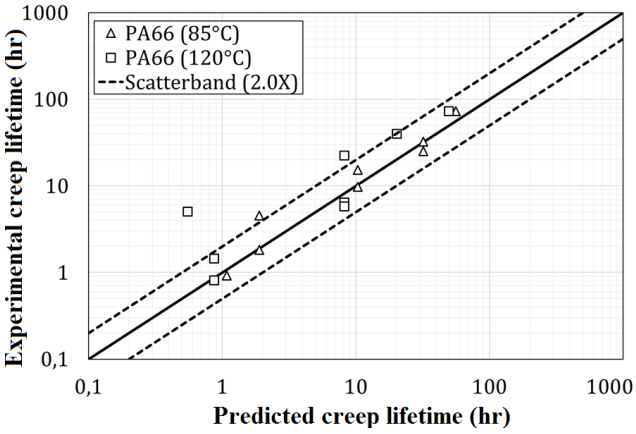

Fig. 11. The experimental creep lifetime versus the predicted creep lifetime for PA66 composites at different temperatures.

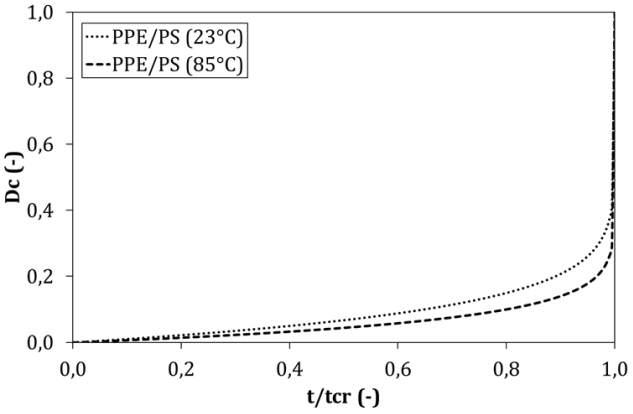

Fig. 12. The creep damage evaluation versus the normalized time for PPE/PS composites at different temperatures.

Table 7
Creep test conditions for PA66 composites.

T (°C)	σ (MPa)	Experimental lifetime [3] (hr)	Predicted lifetime (hr)	Error (%)
85	51.08	0.92	1.08	16.93
85	50.38	1.82	1.90	4.16
85	50.38	4.56	1.90	58.32
85	48.34	9.74	10.34	6.18
85	48.34	15.20	10.34	31.94
85	47.02	24.99	32.00	28.05
85	47.02	32.46	32.00	1.43
85	46.38	73.05	56.27	22.97
120	34.72	73.05	49.70	31.96
120	35.69	40.02	20.22	49.47
120	36.69	22.50	8.23	63.44
120	36.69	6.41	8.23	28.38
120	36.69	5.77	8.23	42.55
120	39.85	5.06	0.55	89.06
120	39.30	1.44	0.87	39.76
120	39.30	0.81	0.87	7.12

Table 8
Creep test conditions for PPE/PS composites.

T (°C)	σ (MPa)	Experimental lifetime [3] (hr)	Predicted lifetime (hr)	Error (%)
23	60.04	0.39	0.27	29.71
23	57.61	0.90	1.24	38.05
23	56.04	3.38	3.43	1.39
23	56.04	3.76	3.43	8.80
23	56.04	6.21	3.43	44.84
23	53.03	22.12	26.06	17.82
23	53.03	25.25	26.06	3.21
23	53.03	50.25	26.06	48.13
85	35.07	1.11	1.09	1.50
85	35.07	1.24	1.09	11.39
85	31.84	6.21	7.22	16.23
85	31.84	7.47	7.22	3.42
85	30.13	17.43	21.20	21.63
85	30.13	27.34	21.20	22.44
85	28.13	80.92	81.55	0.78
85	28.13	97.39	81.55	16.26

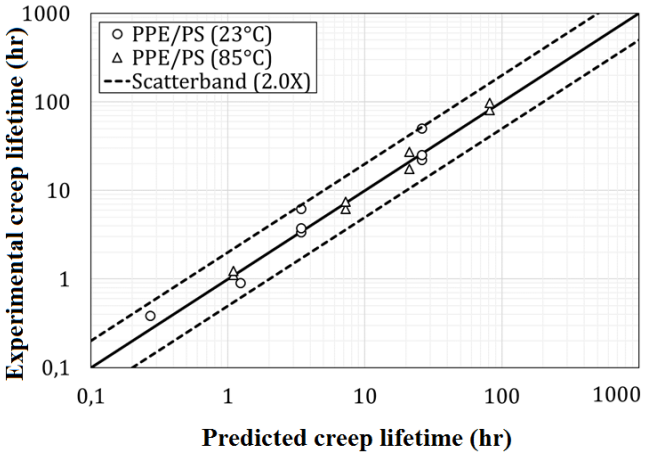

Fig. 13. The experimental creep lifetime versus the predicted creep lifetime for PPE/PS composites at different temperatures.

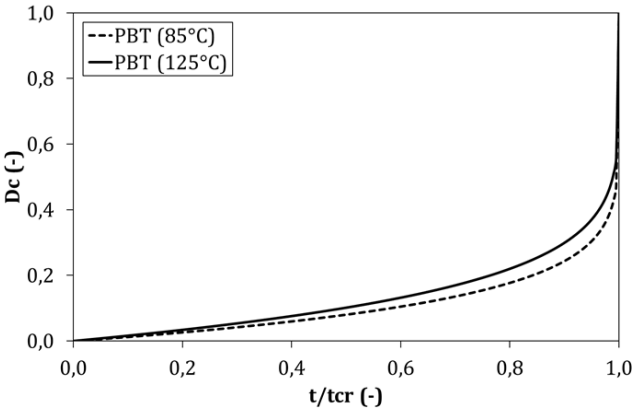

Fig. 14. The creep damage evaluation versus the normalized time for PBT composites at different temperatures.

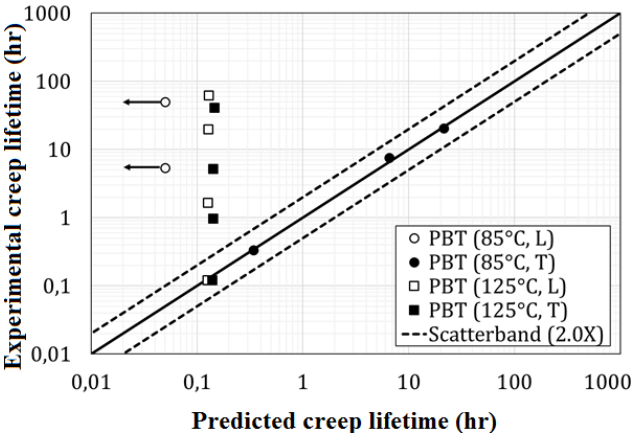

Fig. 15. The experimental creep lifetime versus the predicted creep lifetime for PBT composites at different temperatures.

3.7. PBT Composites

These samples were consisting of polybutylene terephthalate in the matrix and the short glass fiber in the reinforcement phase. Creep tests were conducted at 85°C and 125°C and under different stress levels in transverse and longitudinal directions. Creep tests are described in Table 9. According to data presented in Table 9, the average relative errors for PBT specimens at 85°C and 125°C in transverse directions were 7.05% and 74.65% and in longitudinal directions were 100% and 73.94%, respectively. Maximum relative errors for PBT specimens at 85°C and 125°C in transverse directions were 11.84% and 99.65% and in longitudinal directions were 100% and 99.79%, respectively. These values seemed not to be in a proper range, where some errors had high values, such as 100%. The reason for 100% of the error was that the low number of creep tests for calibrating the CDM model was low. As an example, only one sample and only two samples were considered, respectively for 125°C in the "T" direction and 85°C in the "L" direction of PBT composites. Therefore, for modeling, the direction effect of the material was not considered and then, modeling results for the "L" direction were not in a proper range. Fig. 14 illustrates the creep damage versus the normalized time for PBT composites at different temperatures. Unlike other cases, the higher temperature had higher damage. The experimental creep lifetime versus the predicted creep lifetime, within the 2X scatterband for PBT specimens, can also be seen in Fig. 15.

Based on results for PBT samples, in Table 9 and Fig. 15, the accuracy of modeling was not proper. Since the number of experimental data was not enough; both data in transverse and longitudinal directions were used for the calibration of the model.

3.8. PA6 Composites

Theses samples had polyamide-6 and rubber in the matrix and the short glass fiber in the reinforcement phase. Creep tests were conducted at 85°C and 125°C under different stress levels in both transverse and longitudinal directions. Creep test conditions are detailed in Table 10. According to the data presented in Table 10, the average relative errors for PA6 specimens at 85°C and 125°C in transverse directions were calculated as 53.53% and 50.07% and in longitudinal directions were obtained as 100% and 66.51%, respectively. Maximum relative errors for PA6 specimens at 85°C and 125°C in transverse directions were 96.94% and 96.03% and in longitudinal directions were 100% and 99.42%, respectively. Similarly, the model accuracy was not proper for such a case. These values seemed not to be in a proper range, where some errors had high values, such as 100%. The reason was to consider all data of both directions of the material. Then, modeling results again for the "L" direction of the material were not in a good range.

Table 9
Creep test conditions for PBT composites.

T (°C)	σ (MPa)	Experimental lifetime [3] (hr)	Predicted lifetime (hr)	Error (%)
85, L	53.77	5.34	0.00	100.00
85, L	49.50	49.34	0.00	100.00
85, T	31.84	0.33	0.34	2.68
85, T	29.72	7.50	6.61	11.84
85, T	28.91	20.27	21.61	6.62
125, L	42.53	0.12	0.12	4.33
125, L	39.70	1.64	0.13	92.28
125, L	38.09	19.74	0.13	99.35
125, L	35.07	62.44	0.13	99.79
125, T	23.51	0.12	0.14	16.27
125, L	21.64	0.97	0.14	85.45
125, L	20.77	5.20	0.14	97.25
125, L	18.60	41.08	0.14	99.65

Table 10
Creep test conditions for PA6 composites.

T (°C)	σ (MPa)	Experimental lifetime [3] (hr)	Predicted lifetime (hr)	Error (%)
85, L	68.92	0.19	0.00	100.00
85, L	67.04	19.74	0.00	100.00
85, L	65.22	38.99	0.00	100.00
85, L	61.72	73.05	0.00	100.00
85, T	41.95	0.21	0.10	53.19
85, T	39.70	0.53	0.73	36.07
85, T	37.57	23.71	5.41	77.17
85, T	39.70	23.71	0.73	96.94
85, T	35.55	42.17	40.37	4.27
125, T	56.82	0.24	0.24	1.26
125, T	54.52	23.71	0.27	98.86
125, T	56.82	41.08	0.24	99.42
125, L	30.98	1.37	1.42	4.13
125, L	29.31	42.17	1.68	96.03

Fig. 16 demonstrates the curve of the creep damage evaluation versus the normalized time for PA6 composites at different temperatures. The experimental creep lifetime versus the predicted creep lifetime, within the 2X scatterband for PA6 specimens, can also be seen in Fig. 17. As mentioned, since several data were out of the scatterband, the accuracy of modeling was not proper.

3.9. Temperature-dependant Creep Constants

As noted before, the CDM is a method to predict the creep lifetime. Several researchers have used such an approach to predict the creep behavior of materials. Furthermore, the Levenberg-Marquardt is a common method, which could be used to optimize the CDM relation to find temperature-dependent material constants. Hence, according to creep tests, which were conducted by Eftekahri and Fatemi [5], each of k, A, and r constant parameters would have different values at different conditions and for various composites.

Curves for k, A, and r material constants versus the temperature were drawn for materials, which were tested under at least three temperatures. These materials included PO, PP, and PP-G composites.

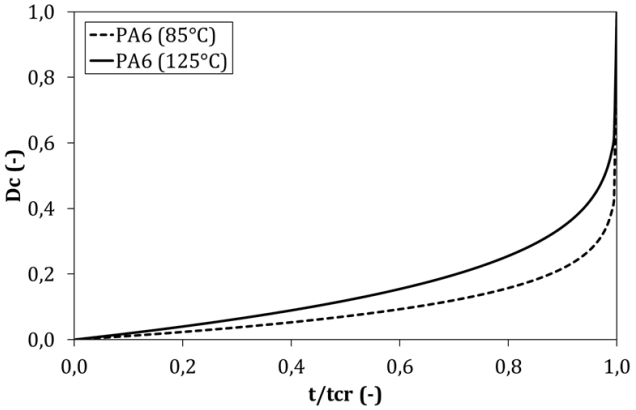

Fig. 16. The creep damage evaluation versus the normalized time for PA6 composites at different temperatures.

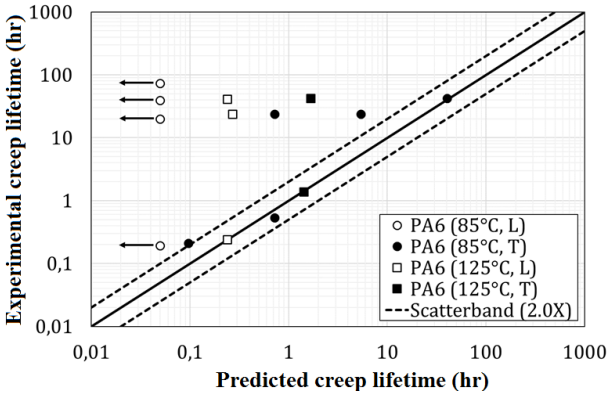

Fig. 17. The experimental creep lifetime versus the predicted creep lifetime for PA6 composites at different temperatures.

Figs. 18, 19, and 20 show the relation between k, A and r material constants and the temperature for PO composites. Figs. 21, 22, and 23 demonstrate the relation between k, A, and r material constants and the temperature for PP composites. The relation between k, A, and r material constants and the temperature for PP-G composites is depicted in Figs. 24, 25, and 26. For such figures, the regression analysis was done based on a linear formulation to find the relation between material constants and the temperature.

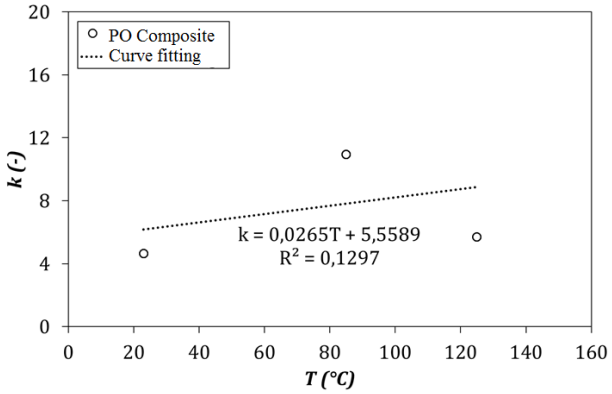

Fig. 18. The relationship between k parameter and the temperature for PO composites.

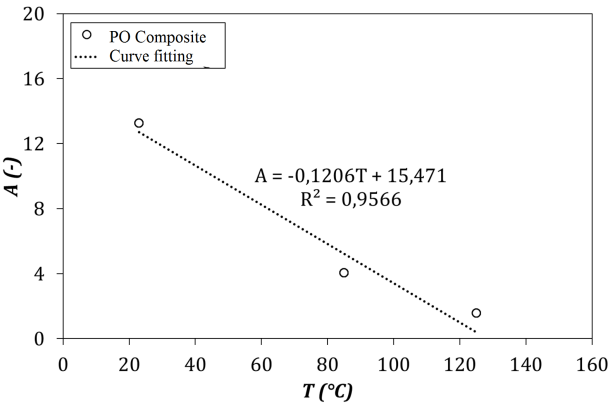

Fig. 19. The relationship between A parameter and the temperature for PO composites.

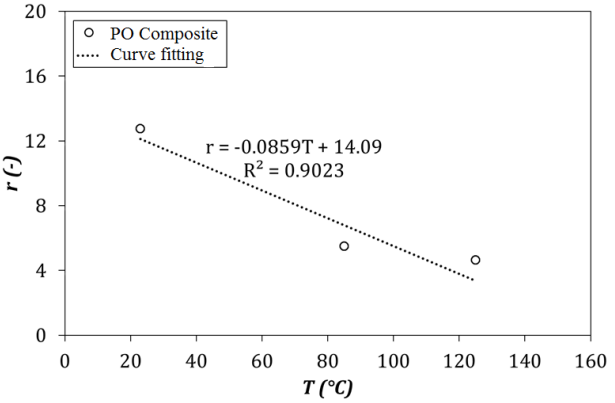

Fig. 20. The relationship between r parameter and the temperature for PO composites.

According to Figs. 18 to 20, the R^2 value for k, A, and r parameters was 12.97%, 95.66%, and 90.23%, respectively. Therefore, it could be concluded that k parameter was not dependent on the temperature. Then, the curve slope was negative in Figs. 19 and 20. It means that by increasing the temperature, A and r material constants decreased, for PO composites. The same behavior could be seen for PP composites. According to Figs. 21 to 23, the R^2 value for k, A, and r parameters was 71.19%, 96.35%, and 99.58%, respectively.

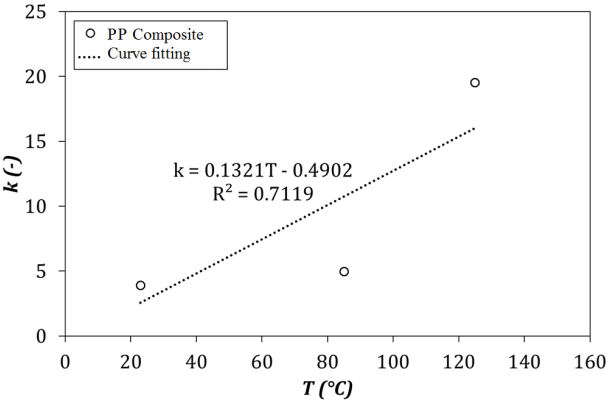

Fig. 21. The relationship between k parameter and the temperature for PP composites.

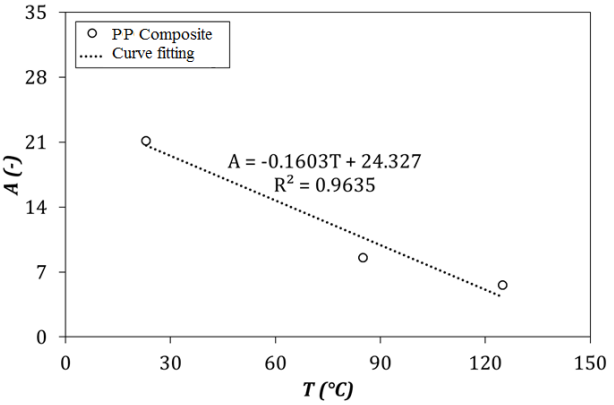

Fig. 22. The relationship between A parameter and the temperature for PP composites.

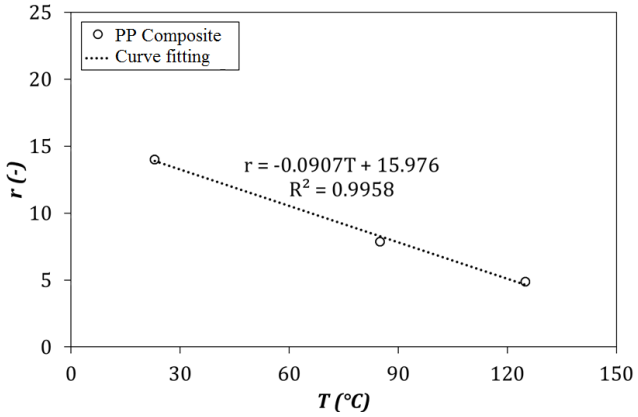

Fig. 23. The relationship between r parameter and the temperature for PP composites.

The relation between k, A, and r material constants and the temperature for PP-G composites can be seen in Figs. 24, 25, and 26. The R^2 value for k, A, and r parameters was 99.03%, 98.81%, and 98.20%, respectively. As could be seen in Fig. 24, the slope was positive. However, the slope in Figs. 25 and 26 was negative.

Comparing the temperature-dependent material constants, found in this study, to some others in other researches [1, 24-26], along with the scatterband which covered all data are presented in Table 11. Such a table could be used for the comparison of material properties of composites, alloys, and superalloys at different temperatures. Such a comparison could verify the obtained results in this research.

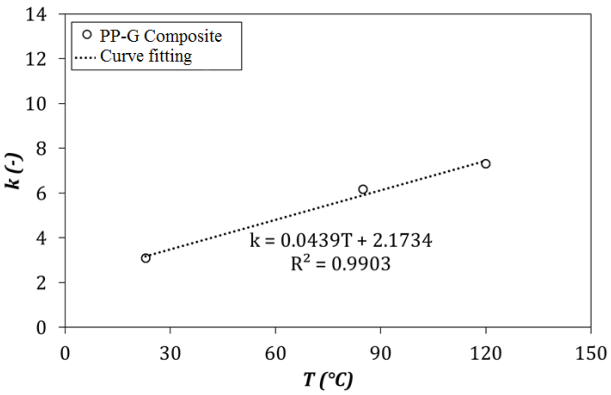

Fig. 24. The relationship between k parameter and the temperature for PP-G composites.

Table 11
Temperature-dependent material constants for different materials at various temperatures

Materials	T (°C)	Material constants			Scatterband
		k	A	r	
PO	23	4.6	13.3	12.7	6.5
PO	85	10.9	4.0	5.5	
PO	125	5.7	1.6	4.7	
PP	23	3.9	21.1	14.0	3.0
PP	85	5.0	8.5	7.9	
PP	125	19.5	5.6	4.9	
PP-T	23	6.8	26.0	18.9	1.5
PP-T	85	7.3	10.3	19.5	
PP-G	23	3.1	40.5	16.5	1.5
PP-G	85	6.2	19.0	10.6	
PP-G	120	7.3	11.4	8.7	
PA66	85	4.8	53.4	4.9	10.0
PA66	120	2.9	40.8	32.6	
PPE/PS	23	8.9	61.7	36.8	2.2
PPE/PS	85	14.2	40.5	19.5	
PBT	85	7.2	32.6	42.9	1.3
PBT	125	5.5	13.5	0.2	
PA6	85	8.4	41.8	36.4	5.0
PA6	125	4.5	62.3	2.9	
Waspaloy [22]	650	20.0	2.1	15.8	2.0
DZ125 [23]	980	5.6	725.2	5.4	2.0
NHT-BJ [23]	980	2.2	423.2	6.4	
HT-BJ [23]	980	3.3	498.8	6.2	
Inconel 713C [1]	850	7.0	700.0	10.5	1.7
Inconel 713C [24]	731	5.02	1521.4	8.12	2.0
Inconel 713C [24]	814	3.34	1255.7	5.89	2.0
Inconel 713C [24]	923	1.37	612.8	4.89	2.0

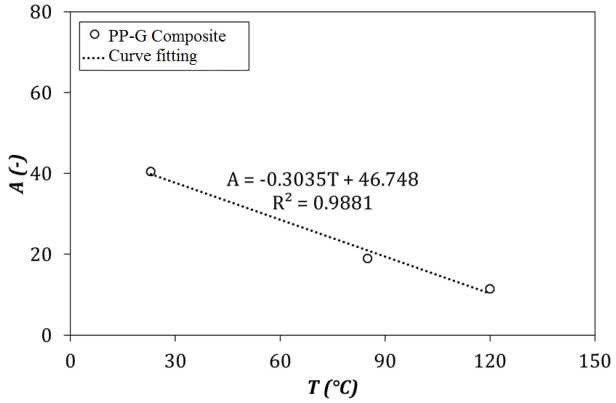

Fig. 25. The relationship between A parameter and the temperature for PP-G composites.

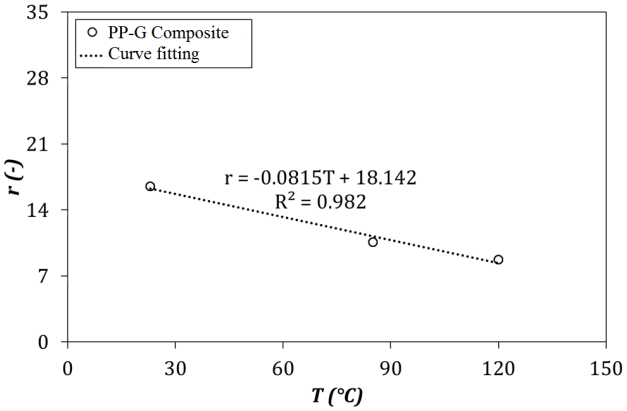

Fig. 26. The relationship between r parameter and the temperature for PP-G composites.

At 23°C, maximum and minimum values of the k parameter were for PPE/PS and PP-G composites, respectively. These values at 85°C were for PPE/PS and PA66 composites, respectively. Similarly, these values at 125°C were for PP and PA6 composites, respectively. Maximum and minimum values of the A parameter were for PPE/PS and PO composites, respectively at 23°C. These values at 85°C were for PA66 and PO composites, respectively. Similarly, these values at 125°C were for PA6 and PO composites, respectively. For the r parameter, maximum and minimum values were for PPE/PS and PO composites, respectively at 23°C. These values at 85°C were for PBT and PA66 composites, respectively. Similarly, these values at 125°C were for PP and PBT composites, respectively. In general, it could be concluded that based on the averaged experimental creep lifetimes, PP-T composites had better creep properties. However, PP composites had the lowest creep lifetime.

The changing limit of k, A, and r parameters for all composites in this article are presented in Table 12, comparing to the literature [1, 22-26]. This table verified the obtained values for such parameters. Consequently, creep constants were found well for PP-T, PP-G, PPE/PS, and PBT composites, based on obtained results for the scatterband.

The optimization for PO, PP, PA66, and PA6 composites was not good enough. However, the optimization process could be affected by materials and creep test conditions, especially the test number. It should be noted that relative errors for PBT composites were high and the model was not proper.

Table 12
The changing limit of material constants.

Parameter	Present study		Other references [1, 21-24]	
	Minimum	Maximum	Minimum	Maximum
k	2.9	19.5	1.7	20.0
A	1.6	62.3	2.1	15.2
r	0.2	42.9	4.9	15.8

4. Conclusions

In this article, creep modeling of some polymer matrix composites, reinforced by the short glass fiber and talc, was investigated. The CDM approach was proposed to predict the creep lifetime of composites. Significant conclusions of this study could be described as follows,

- Except for some special cases, other predicted creep lifetimes had a good agreement with experimental results and almost the 2X scatterband could cover all data.
- As seen in damage curves, because of the dependency of damage parameter on the k parameter, it could be noted that the damage curve slope increased due to an increase in the k parameter.
- Except for PA66, PBT, and PA6 composites, in other cases, the lower temperature had higher damage.
- In general, the value of k parameter increased, when the temperature increased for PO, PP, PP-T, PP-G, and PPE/PS specimens, except for PA66, PBT, and PA6 samples.
- The value of the A parameter for all specimens (except PA6 composites) decreased by increasing the temperature. Moreover, the value of the r parameter for all specimens (except PP-T composites) decreased due to the temperature increase.

- Consequently, the CDM model was appropriate to estimate the creep lifetime of PP-T, PP-G, PPE/PS composites, based on lower scatterband and lower relative error. In other words, the Levenberg-Marquardt method could properly optimize material constants for such composites.

References

[1] H. Bahmanabadi, S. Rezanezhad, M. Azadi, M. Azadi, Characterization of creep damage and lifetime in Inconel-713C nickel-based superalloy by stress-based, strain/strain rate-based and continuum damage mechanics models, Mater. Res. Express, 5(2) (2018) 26509.

[2] N. Habibi, S. Samawati, O. Ahmadi, Creep analysis of the FGM cylinder under steady-state symmetric loading, J. Stress Anal., 1(1) (2016) 9-21.

[3] M. Saadatfar, Effect of hygrothermal environmental conditions on the time-dependent creep response of functionally graded magneto-electro-elastic hollow sphere, J. Stress Anal., 4(1) (2019) 27-41.

[4] V.S. Chevali, D.R. Dean, G.M. Janowski, Flexural creep behavior of discontinuous thermoplastic composites: Non-linear viscoelastic modeling and time-temperature-stress superposition, Composites Part A, 40(6-7) (2009) 870-877.

[5] M. Eftekhari, A. Fatemi, Creep behavior and modeling of neat, talc-filled, and short glass fiber reinforced thermoplastics, Composite Part B, 97 (2016) 68-83.

[6] S. Rwawiire, B. Tomkova, J. Wiener, J. Militky, A. Kasedde, B.M. Kale, A. Jabbar, Short-term creep of barkcloth reinforced laminar epoxy composites, Composite Part B, 103 (2016) 131-138.

[7] Y. Du, N. Yan, M. T. Kortschot, An experimental study of creep behavior of lightweight natural fiber-reinforced polymer composite/honeycomb core sandwich panels, Compos. Struct., 106 (2013) 160-166.

[8] R. Song, A.H. Muliana, A. Palazotto, An empirical approach to evaluate creep responses in polymers and polymeric composites and determination of design stresses, Compos. Struct., 148 (2016) 207-223.

[9] T. Pulngern, T. Chitsamran, S. Chucheepsakul, V. Rosarpitak, S. Patcharaphun, N, Sombatsompop, Effect of temperature on mechanical properties and creep responses for wood/PVC composites, Constr. Build. Mater., 111 (2016) 191-198.

[10] A. Jabbar, J. Militky, B.M. Kale, S. Rwawiire, Y. Nawab, V. Baheti, Modeling and analysis of the creep behavior of jute/green epoxy composites incorporated with chemically treated pulverized nano/micro jute fibers, Ind. Crops Prod., 84 (2016) 230-240.

[11] P.K. Dutta, D. Hui, Creep rupture of a GFRP composite at elevated temperatures, Ind. Crops Prod., 76(1-3) (2000) 153-161.

[12] A. Gupta, J. Raghavan, Creep of plain weave polymer matrix composites under on-axis and off-axis loading, Composites Part A, 41(9) (2010) 1289-1300.

[13] S. Mortazavian, A. Fatemi, Fatigue of short fiber thermoplastic composites: A review of recent experimental results and analysis, Int. J. Fatigue, 102 (2017) 171-183.

[14] S.K. Ghosh, R.K. Prusty, D.K. Rathore, B.C. Ray, Creep behaviour of graphite oxide nanoplates embedded glass fiber/epoxy composites: Emphasizing the role of temperature and stress, Composites Part A, 102 (2017) 166-177.

[15] A. Pegoretti, T. Ricco, Creep crack growth in a short glass fibres reinforced polypropylene composite, J. Mater. Sci., 36(19) (2001) 4637-4641.

[16] F. Su, P. Huang, J. Wu, B. Chen, Q. Wang, R. Yao, T. Li, X. Pan, Creep behavior of C/SiC composite in hot oxidizing atmosphere and its mechanism, Ceram. Int., 43(12) (2017) 9355-9362.

[17] R. Cano-Crespo, B. M. Moshtaghioun, D. Gomez-Garcia, A. Dominguez-Rodriguez, R. Moreno, High-temperature creep of carbon nanofiber-reinforced and graphene oxide-reinforced alumina composites sintered by spark plasma sintering, Ceram. Int., 43(9) (2017) 7136-7141.

[18] A. Plaseied, A. Fatemi, Tensile creep and deformation modeling of vinyl ester polymer and its nanocomposite, J. Reinf. Plast. Compos., 28(14) (2009) 1775-1788.

[19] K.C. Hung, T.L. Wu, Y.L. Chen, J.H. Wu, Assessing the effect of wood acetylation on mechanical properties and extended creep behavior of wood/recycled-polypropylene composites, Constr. Build. Mater., 108 (2016) 139-145.

[20] J. Raghavan, M. Meshii, Creep of polymer composites, Compos. Sci. Technol., 57(12) (1998) 1673-1688.

[21] J. Militky, A. Jabbar, Comparative evaluation of fiber treatments on the creep behavior of jute/green epoxy composites, Composite Part B, 80 (2015) 361-368.

[22] ASTM D2990-09, Standard test methods for tensile, compressive and flexural creep and creep-rupture of plastics, West Conshohocken, PA: ASTM International, (2009).

[23] H. Bahmanabadi, Evaluation of Continuum Damage Mechanics in Inconel 713C Nickel-based Superalloy under Force-Controlled Creep Loading, BSc. Thesis, Iran: Semnan University (2016).

[24] T.W. Kim, D.H. Kang, J.T. Yeom, N.K. Park, Continuum damage mechanics-based creep-fatigue-interacted life prediction of nickel-based superalloy at high temperature, Scr. Mater., 57(12) (2007) 1149-1152.

[25] D. Shi, C. Dong, X. Yang, Y. Sun, J. Wang, J. Liu, Creep and fatigue lifetime analysis of directionally solidified superalloy and its brazed joints based on continuum damage mechanics at elevated temperature, Mater. Des., 45 (2013) 643-652.

[26] Engineering Properties of Alloy 713C, Technical Literature, No. 337, Nickel Institute, Belgium.